ACS APPLIED MATERIALS & INTERFACES

Research Article

www.acsami.org

Photostability of Phosphonate-Derivatized, Ru^{II} Polypyridyl Complexes on Metal Oxide Surfaces

Kenneth Hanson, M. Kyle Brennaman, Hanlin Luo, Christopher R. K. Glasson, Javier J. Concepcion, Wenjing Song, and Thomas J. Meyer*

Department of Chemistry, University of North Carolina at Chapel Hill, Chapel Hill, North Carolina 27599, United States

Supporting Information

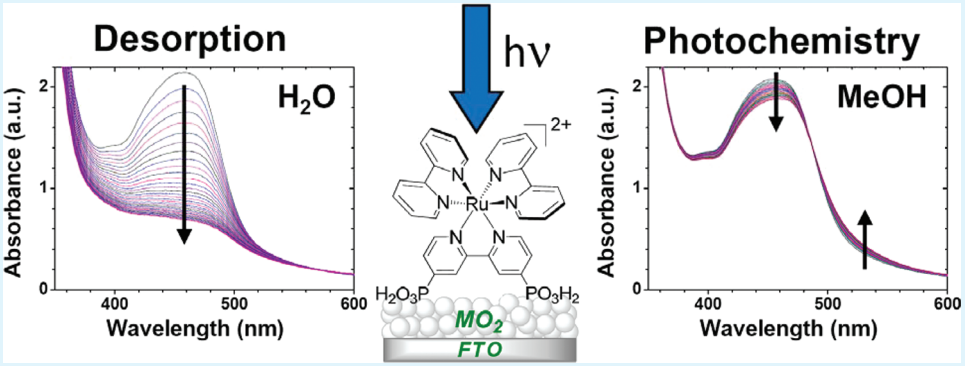

ABSTRACT: The photostability of $[Ru^{II}(bpy)_2(4,4'\text{-}(PO_3H_2)_2bpy)]Cl_2$ (bpy = 4,4′-bipyridine) on nanocrystalline TiO_2 and ZrO_2 films was investigated using a standard measurement protocol. Stability was evaluated by monitoring visible light absorbance spectral changes, in real time, during 455 nm photolysis (30 nm fwhm, 475 mW/cm^2) in a variety of conditions relevant to dye-sensitized solar cells and dye-sensitized photoelectrosynthesis cells. Desorption (k_{des}) and photochemical (k_{chem}) processes were observed and found to be dependent upon solvent, anion, semiconductor, and presence of oxygen. Both processes are affected by oxygen with k_{des} and k_{photo} noticeably smaller in argon saturated solution. Desorption was strongly solvent and pH dependent with desorption rates increasing in the order: methanol (MeOH) ≈ acetonitrile (MeCN) < propylene carbonate (PC) < pH 1 ≪ pH 7. Photochemistry occurred in MeOH and PC but not in aqueous, 0.1 M $HClO_4$ and MeCN. The anion and solvent dependence of k_{photo} strongly suggests the photoreaction involves ligand substitution initiated by population of metal centered d-d states. The relative stability of $-PO_3H_2$- versus −COOH-substituted $[Ru^{II}(bpy)_3]^{2+}$ was also quantitatively established.

KEYWORDS: *dye-sensitized solar cell (DSSC), dye-sensitized photoelectrosynthesis cell (DSPEC), ruthenium polypyridine, photostability, desorption, photochemistry*

INTRODUCTION

Ruthenium(II) polypryridyl light-absorbing complexes bound to metal oxide semiconductor nanoparticles are often at the heart of functional dye-sensitized solar cells (DSSCs) and dye-sensitized photoelectrosynthesis cells (DSPECs).[1] Even so, there is minimal quantitative information about the stability of the resulting interfaces.[2] The current technological drive for DSSC and DSPEC commercialization requires an assessment of interface stability under a variety of operating conditions.[3,4]

There are several reports that either briefly mention or exclusively study the stability of surface-bound chromophores when immersed in solution in the dark[5,6] or by performing thermal stability measurements.[3,7] Photostability studies of ruthenium polypyridyl chromophores on metal oxide surfaces have been reported but are typically limited to absorption spectral measurements of thin films before and after irradiation.[8−10]

Under simulated sun exposure, Uam et al. observed a steady decrease in DSSC short-circuit photocurrent density correlated with a decrease in surface absorbance and an increase in ruthenium concentration in the external solution.[11] Observations of this kind make it clear that surface stability can be pivotal in maximizing and maintaining device performance.[12,13] Unfortunately, detailed mechanistic studies, beyond simple observation of device performance changes are limited,[2,14] providing little insight into the chemical pathways responsible for degradation (thermal decomposition, photodegradation, etc.).

In this report, we investigate the photostability of ruthenium polypyridyl chromophores on metal oxide films by monitoring, in real time, changes in visible light absorbance under a variety

Received: December 5, 2011
Accepted: February 8, 2012
Published: February 8, 2012

of conditions relevant to solar energy conversion. $[Ru^{II}(bpy)_2(4,4'\text{-}(PO_3H_2)_2bpy)]Cl_2$ (**RuP**) and $[Ru^{II}(bpy)_2(4,4'\text{-}(COOH)_2bpy)]Cl_2$ (**RuC**) (Figure 1) are

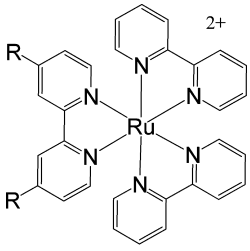

Figure 1. Structures of $[Ru(bpy)_2(4,4'\text{-}(PO_3H_2)_2bpy)]^{2+}$ (**RuP**) and $[Ru(bpy)_2(4,4'\text{-}(COOH)_2bpy)]^{2+}$ (**RuC**).

used as example chromophore/surface-bound light absorbers. The effects of variations in electrolyte, metal oxide substrate, solvent, pH, and presence of oxygen on desorption/photoreaction rates are systematically investigated by application of a standardized measurement protocol. This study includes both aqueous and organic solvents to gain an understanding of the factors that influence the stability of chromophore molecules on semiconductor nanoparticles under conditions relevant to both DSPEC and DSSC applications.

EXPERIMENTAL SECTION

Sample Preparation. Nano-TiO_2[15] films and nano-ZrO_2[16] films, typically 7 μm thick, coating an area of 11 mm × 25 mm on top of FTO (fluorine-doped SnO_2) glass were prepared according to previously published procedures. **RuP** and **RuC** were synthesized as their chloride salts according to previously published procedures.[5] All semiconductor film coated electrodes were dye-sensitized by soaking in 150 μM **RuP** in a 0.1 M $HClO_4$ aqueous solution or 150 μM **RuC** in ethanol overnight followed by soaking for an additional 12 h in 0.1 M $HClO_4$ or ethanol to remove any possible **RuP**/**RuC** aggregates. In accord with previous reports, the 150 μM sensitizer solution concentration results in complete monolayer coverage of the metal oxide films.[17] Sensitization occurred in the dark.

Photostability Measurements. Photostability measurements were performed by using the apparatus in Figure S1 in the Supporting Information. The light from a Royal Blue (455 nm, fwhm ~30 nm, 475 mW/cm^2) Mounted high power LED (Thorlabs, Inc., M455L2) powered by a T-Cube LED driver (Thorlabs, Inc., LEDD1B) was focused to a 2.5 mm diameter spot size by a focusing beam probe (Newport Corp. 77646) outfitted with a second lens (Newport, Corp 41230). Light output was directed onto the derivatized thin films placed at 45° in a standard 10 mm path length cuvette containing 5 mL of the solutions of interest. The illumination spot was adjusted to coincide both with the thin films and the perpendicular beam path of a Varian Cary 50 UV−vis spectrophotometer. The absorption spectrum (360−800 nm) of the film was obtained every 15 min during 16 h of illumination. The incident light intensity was measured using a thermopile detector (Newport Corp 1918-C meter and 818P-020-12 detector). The solution temperature, 22 ± 2 °C, was consistent throughout the duration of the experiment.

RESULTS

1. Water. For **RuP** in aqueous conditions, strong $\pi-\pi^*$ transitions below 350 nm and lower energy metal-to-ligand charge-transfer (MLCT) transitions from 400 to 500 nm can be observed. Due to the light absorption and scatter of TiO_2 and ZrO_2, visible absorption changes of only the MLCT band were monitored (350−700 nm). As shown in Figure 2a, there were

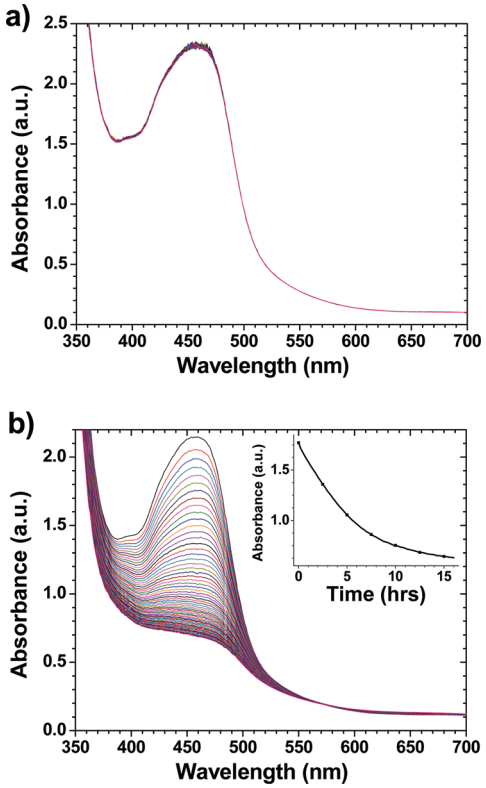

Figure 2. Changes in the absorption spectrum of **RuP** on TiO_2 in 0.1 M $HClO_4$ (a) without and (b) with irradiation (475 mW/cm^2). Inset b: Absorbance at 480 nm versus time.

no spectral changes for a film of **RuP** on TiO_2, in 0.1 M aqueous $HClO_4$ (pH 1) in the dark (room temperature, atm) over a 16 h period. Under the same conditions, but with 455 nm constant irradiation (fwhm ~30 nm, 475 mW/cm^2), a gradual decrease in the MLCT absorbance was observed from 400 to 500 nm (Figure 2b). Removal of the slide from the solution revealed bare TiO_2 over the photolyzed area (~2.5 mm diameter) consistent with desorption or decomposition of **RuP** on TiO_2. The exposed white area was not simply due to remnant photo-oxidized Ru(III) complex on the surface because electrochemical and chemical reduction (ascorbic acid or sodium dithionite in H_2O) of the slide did not result in the return of color expected for the regeneration of Ru(II).

The rate of MLCT absorption loss was similar from 375 to 500 nm. Single wavelength kinetics was evaluated at 480 nm because it is an isosbestic point of the photochemical reaction (vida infra). The absorption-time traces at 480 nm (Figure 2b, inset) could be satisfactorily fit with the biexponential function in eq 1. The multiexponential nature of the absorption changes under illumination could arise from a variety of competing desorption/decomposition pathways and/or, as noted for surface electron transfer kinetics, local inhomogeneities in the metal-oxide surface structure.[12,18] For comparative purposes, the results of the multiexponential analysis were represented by a single rate constant, the disappearance or desorption rate constant, k_{des}, by calculating the weighted average lifetime ($\langle\tau\rangle$) by application of eq 2. In eq 2, A_i and τ_i are the contributions to the absorbance amplitude and lifetime of component *i*.

$$k_{obs} = A_1 e^{-k_1 t} + A_2 e^{-k_2 t} \quad (1)$$

$$1/k_{des} = \langle \tau \rangle = \Sigma A_i \tau_i^2 / \Sigma A_i \tau \quad (2)$$

In 0.1 M $HClO_4$, k_{des} = 5.0 ± 0.2 × 10^{-5} s^{-1} for the disappearance of **RuP** on TiO_2 under the photolysis conditions described above. The k_{des} in 0.1 M $HClO_4$ was reproducible (±0.2 × 10^{-5} s^{-1}) for several samples prepared from different batches of TiO_2 and **RuP** loading solutions. The dynamics of surface loss are proportional to light intensity from 50 to 475 mW/cm^2 as shown in Table S1 and Figure S2 in the Supporting Information. Further experiments were conducted at the highest incident irradiation.

The effect of increasing pH, at pH 3, 5, and 7 with $HClO_4$ in 0.1 M $LiClO_4$, was also investigated, (see Figure S3 in the Supporting Information). Under irradiation k_{des} increased from pH 1 (5.0 × 10^{-5} s^{-1}) to pH 3 (8.6 × 10^{-5} s^{-1}). At pH 5 and 7 (see Figure S3c, d in the Supporting Information), no further change in absorption occurred after the first 3–4 h with continued photolysis. Visual examination of the slides after photolysis at pH 5 and 7 reveal that in addition to the bare TiO_2 at the site of photolysis, color loss was notable on the entire surface albeit much less pronounced than in the photolyzed area. UV–visible measurements of the pH 5 and pH 7 solutions after photolysis revealed the presence of **RuP** in the external solution consistent with a desorption mechanism. Because of competing absorbance of **RuP** in the pH 5 and 7 solutions, the kinetics of **RuP** desorption from TiO_2 were not analyzed quantitatively.

Under the conditions of our experiments, injection yields for **RuP** on TiO_2 vary from 1.0 at pH 1 to 0.7 at pH 5.[16] The decreased injection yield at higher pH is attributed to the Nernstian pH dependence on the conduction band energy. The more negative conduction band at higher pH hinders excited state electron injection from **RuP** into TiO_2.[17] ZrO_2 has a comparable surface structure but the conduction band is ~1 eV higher in energy, too high for excited state injection from **RuP**.[19] Under our standard photolysis conditions, k_{des} on ZrO_2 (0.4 × 10^{-5} s^{-1}) is an order of magnitude slower than on TiO_2 (5.0 × 10^{-5} s^{-1}). The rate of desorption is decreased by 20% on TiO_2 and 50% on ZrO_2 by deaeration with argon or nitrogen. Interestingly, surface loss kinetics under argon and nitrogen follow zero order kinetics. Although this observation points to a contribution from oxygen (see below), k_{des} in a pure oxygen atmosphere at pH 1 was the same (4.9 × 10^{-5} s^{-1}) as in air. A summary of these results is given in Table 1.

2. Acetonitrile. Acetonitrile is a common solvent for DSSCs. Desorption of **RuP** from TiO_2 under standard photolysis conditions was an order of magnitude slower in MeCN than in water with k_{des} = 0.81 × 10^{-5} s^{-1}. The addition of 0.05 or 0.1 M $LiClO_4$ had no influence on the desorption rate (k_{des} = 0.80 × 10^{-5} s^{-1}). The addition of water accelerated desorption with k_{des} increasing roughly linearly with added water up to 5% v:v (2.8 M) but then leveling off above 20% (>11.1 M) at k_{des} = 5.0 × 10^{-5} s^{-1} (see Figure S4 and Table S1 in the Supporting Information). These observations are qualitatively consistent with earlier results and indicative of a partitioning equilibrium of water between solvent and the TiO_2 film. The high affinity of water for TiO_2 films has been documented.[20]

3. Methanol. A different result was obtained upon photolysis of TiO_2-**RuP** in methanol (Figure 3). In addition to the decrease of the visible MLCT band from 400 to 500 nm, an absorption increase occurred from 490 to 700 nm. In solutions that inhibit desorption (vide infra), absorption changes with time occurred with a well-defined isosbestic point at ~480 nm consistent with conversion to a new surface bound species. Photochemical desorption kinetics were monitored at 480 nm and photochemical conversion (k_{photo}) at 550 nm. Absorbance-time traces at both 480 and 550 nm (Figure 3, inset) were fit to the biexponential expression in eq 1 with weighted averages for k_{des} and k_{photo} reported in Table 2.

Desorption of **RuP** from TiO_2 in methanol is slower (0.9 × 10^{-5} s^{-1}) than in 0.1 M $HClO_4$ (5.0 × 10^{-5} s^{-1}) but comparable in rate to acetonitrile (0.8 × 10^{-5} s^{-1}) (Table 1). In argon deaerated solutions, desorption becomes negligible over the 16 h photolysis period with k_{des} < 0.01 × 10^{-5} s^{-1}. Unlike

Table 1. Summary of Rate Constants for Desorption (k_{des}) and Photochemistry (k_{photo}) for MO_2–RuP with Variations in Medium, Metal Oxide, and Atmosphere[a]

solvent	MO_2	atm vs Ar	k_{des} (× 10^{-5} s^{-1})	k_{photo} (× 10^{-5} s^{-1})
0.1 M $HClO_4$	TiO_2	atm	5.0	
	TiO_2	Ar	1.0[b]	
	ZrO_2	atm	0.4	
	ZrO_2	Ar	0.2[b]	
MeCN	TiO_2	atm	0.8	
	TiO_2	Ar	0.16[b]	
MeOH	TiO_2	atm	0.9	3.3
	TiO_2	Ar	<0.01	2.2
	ZrO_2	atm	0.7	1.3
	ZrO_2	Ar	<0.01	1.1
PC	TiO_2	atm	1.7	3.0
	TiO_2	Ar	<0.01	2.0

[a]Under 475 mW/cm^2. [b]Zero-order kinetics, M s^{-1}.

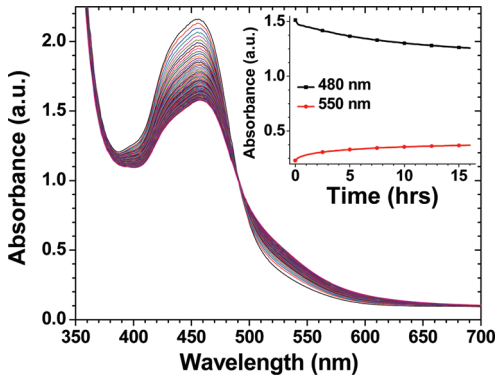

Figure 3. Changes in the absorption spectrum of TiO_2–**RuP** in methanol. Inset: Absorbance–time traces at 480 and 550 nm.

Table 2. Desorption (k_{des}) and Photochemical (k_{photo}) Rate Constants for RuP–TiO_2 in Methanol with and without Added Salts (0.1 M)[a]

salt	k_{des} (× 10^{-5} s^{-1})	k_{photo} (× 10^{-5} s^{-1})
	0.9	3.3
$LiOOCCH_3$	10.4	3.1
LiCl	<0.01	2.0
$LiSO_3CF_3$	<0.01	0.6
$LiPF_6$	<0.01	0.2
$LiClO_4$	<0.01	1.3
$NaClO_4$	<0.01	1.0
$Mg(ClO_4)_2$	<0.01	1.1

[a]Under 475 mW/cm^2 illumination, in air at room temperature.

0.1 M $HClO_4$, k_{des} in methanol is comparable on both TiO_2 and ZrO_2.

From the data in Table 2, with the exception of $LiOOCCH_3$ (k_{des} =0.9 × 10^{-5} s^{-1}), the addition of LiX salts (X = Cl^-, $SO_3CF_3^-$, PF_6^- and ClO_4^-) significantly retards desorption to k_{des}< 0.01 × 10^{-5} s^{-1}. Added salts similarly hindered growth of the new species with k_{photo} decreasing in the order H_3CCOO^- < Cl^- < ClO_4^- < $SO_3CF_3^-$ < PF_6^- relative to neat MeOH. Changes in cation in ClO_4^- salts had a negligible effect for Li^+, Na^+, and Mg^{2+}.

With desorption hindered in the presence of 0.1 M $LiClO_4$, the rate of absorbance growth from 480 to 700 nm approximately matched the absorption decrease from 400 to 480 nm during 24 h of photolysis (Figure 4a). Spectral

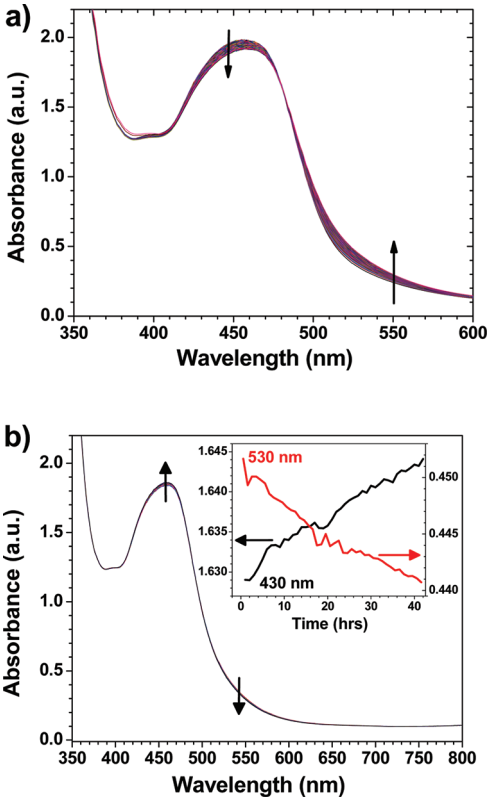

Figure 4. Changes in the absorption spectrum of TiO_2–**RuP** in 0.1 M $LiClO_4$ methanol taken: (a) every 15 min for 16 h during irradiation (475 mW/cm^2) and (b) every 60 min for 42 h beginning at the end of the photolysis period. Inset: Absorbance–time traces at 430 and 530 nm.

monitoring over the subsequent 42 h in the dark reveals a complementary increase and decrease in absorbance at 430 and 530 nm, respectively (inset in Figure 4b). The absorbance change in the dark is attributed to the photochemical reaction being at least partially reversible albeit significantly slower than the forward reaction.

It is worth noting that similar spectral shifts as those described above, a decrease of the visible MLCT band from 400 to 490 nm and an absorption increase occurred from 490 to 700 nm, was reported by Caramori et al. when $[Ru^{II}(4,4'\text{-}(PO_3H_2)_2)bpy)_3]_2^{2+}$ on TiO_2 was irradiated in 0.1M$LiClO_4$ in an 8:2 water/isopropyl alcohol electrolyte.[8]

4. Propylene Carbonate. Propylene carbonate (PC) and propylene carbonate-ethylene carbonate mixtures have been shown to be useful solvents in water oxidation catalysis.[7] The photochemical behavior of TiO_2-**RuP** in PC was similar to methanol in both desorption (k_{des} = 1.7 × 10^{-5} s^{-1}) and photochemistry (k_{photo} = 3.0 × 10^{-5} s^{-1}). Changes with argon deaeration were also similar with k_{des} < 0.01 × 10^{-5} s^{-1} and k_{photo} decreased to 2.0 × 10^{-5} s^{-1}. The addition of $LiSO_3CF_3$ (0.1 M) to the aerated PC solution also greatly decreased both desorption (k_{des} < 0.01 × 10^{-5} s^{-1}) and photochemistry (k_{photo} = 0.1 × 10^{-5} s^{-1}). Attempts to identify the small amount of the photoproduct by NMR were unsuccessful (see the Supporting Information).

5. PO_3H_2 vs COOH Binding. Relative stabilities of the phosphonate, $[Ru^{II}(bpy)_2(4,4'\text{-}(PO_3H_2)_2bpy)]^{2+}$ (**RuP**), and carboxylate, $[Ru^{II}(bpy)_2(4,4'\text{-}(COOH)_2bpy)]^{2+}$ (**RuC**), derivatives on TiO_2 were also compared with the results summarized in Table 3. In 0.1 M $HClO_4$ aqueous solution

Table 3. Comparisons of k_{des} for TiO_2–RuP and TiO_2–RuC in Various Conditions under Irradiation unless Otherwise Noted[a]

		k_{des} (10^{-5} s^{-1})	
solvent	atm vs Ar	**RuC**	**RuP**
0.1 M $HClO_4$[b]	atm	8.5	<0.01
MeCN	atm	3.8	0.8
	Ar[c]	1.1	0.3
MeOH	atm	4.9	0.9

[a]Room temperature, 475 mW/cm^2. [b]Without irradiation. [c]Zero order with respect to **RuP**/**RuC**, M s^{-1}.

(pH 1) with no irradiation, desorption of **RuC** from TiO_2 (k_{des} = 8.5 × 10^{-5} s^{-1}) is significantly more rapid than TiO_2–**RuP** consistent with the documented aqueous solution lability of carboxylated ruthenium polypyridyl complexes.[6,21,22] In both acetonitrile and methanol, desorption of **RuC** is more facile than **RuP** by a factor of ~5. With argon deaeration in acetonitrile k_{des} decreases from 3.8 × 10^{-5} s^{-1} to 1.1 × 10^{-5} s^{-1}, a decrease comparable to that found for **RuP**. Desorption of **RuC** under argon occurred with zero-order kinetics.

DISCUSSION

In this study, our intent was to explore the variables that affect the stability of surface-bound ruthenium(II) polypryridyl chromophores under conditions appropriate for DSSC and DSPEC operation. In the absence of light, metal oxide bound **RuP** is unaltered over a 16 h interval. Under irradiation both desorption and photochemistry were observed, dependent upon conditions. On nanocrystalline TiO_2 and ZrO_2 surfaces both processes were active despite the photoproduction of two different transient surface-bound species, Ru^{III} on TiO_2 due to electron injection and Ru^{II}* on ZrO_2.

Higher rates of desorption and photochemistry were observed on TiO_2 than on ZrO_2. Both processes are dependent on oxygen with k_{des} and k_{photo} noticeably decreased in magnitude in argon deaerated solutions. Desorption is strongly solvent and pH dependent with desorption rates increasing in the order: MeOH≈MeCN < PC < pH 1 ≪ pH 7. Photochemical conversion was also found to be strongly solvent dependent with the photoproduct observed in MeOH and PC but not in 0.1 M $HClO_4$ and MeCN. The anion and solvent dependence of k_{photo} strongly suggests that the photoreaction involves ligand substitution initiated by

dx.doi.org/10.1021/am201717x | ACS Appl. Mater. Interfaces 2012, 4, 1462–1469

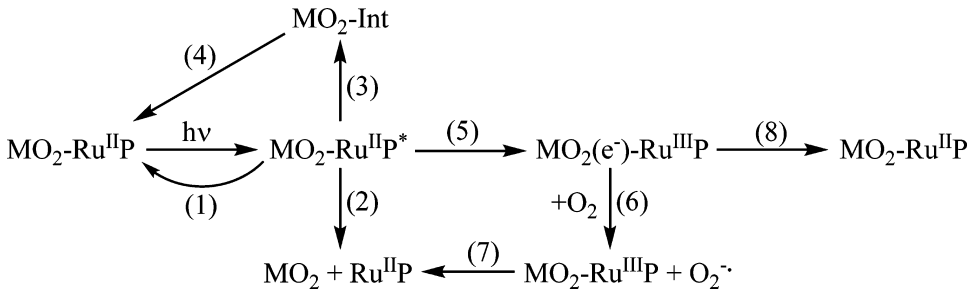

Figure 5. Reaction scheme for **RuP** on MO_2 (MO_2–$Ru^{II}P$) illustrating: (1) radiative and nonradiative relaxation, (2 + 7) desorption, (3) excited state chemistry, (4) thermal reversibility, (5) excited state electron injection, (6) electron transfer reduction of O_2 to give $O_2^{-\cdot}$, and (8) back electron transfer.

population of metal centered d–d states as observed earlier in nonpolar solvents.[23]

There is enough information from these studies to suggest the origins of photoinitiated loss and photochemistry for **RuP** on the oxide surfaces. The processes that occur are summarized in Figure 5.

Desorption from ZrO_2. The high conduction band of ZrO_2 (~−1.4 V vs NHE, pH 7) inhibits excited state electron injection (5).[19] MLCT excitation results in MO_2–$Ru^{II}P$* without complications from injection, process (5) in Figure 5. In addition to radiative and nonradiative relaxation (1), on ZrO_2–**RuP**, both desorption (2) and photochemistry (3) occur.

In the absence of oxygen, k_{des} was found to be zero-order with respect to chromophore in water at pH 1. Zero-order desorption kinetics point to a rate limiting step not involving absorption by **RuP**. Its origin is not known but may be symptomatic of a localized heating process that assists subsequent thermal loss from the surface. At the excitation energy of 455 nm (2.72 eV), there may also be a contribution from two-photon band gap excitation[24] resulting in photo-induced superhydrophilicity or another mechanism.[25] However, the linear dependence of k_{des} on light intensity (see Table S1 and Figure S2 in the Supporting Information) suggests that a two-photon event is not the dominant desorption mechanism. With added oxygen the desorption time scale is halved and kinetics become first order in **RuP** on ZrO_2 in both methanol and 0.1 M $HClO_4$. The excited-state lifetime with added O_2 is diminished, which is attributable to oxygen quenching to give singlet O_2 ($^1O_2$).[26] Under these conditions, ZrO_2–$Ru^{II}P$* sensitization of $^3O_2$ to $^1O_2$ and singlet oxygen attack on surface binding sites may explain the enhanced desorption rate.[27]

Photochemistry on ZrO_2. In contrast to water, where only decreases in absorption and loss of complex were observed, in methanol, photolysis of ZrO_2–$Ru^{II}P$ results in both desorption and spectral shifts. The spectral changes are significant (>20 nm) but comparable to previously reported $[Ru^{II}(bpy)_2(py)X]^+$ species.[23,28] In solution, photochemical ligand exchange on $[Ru^{II}(bpy)_3]^{2+}$ is known to occur suggesting a similar origin for process (3) on ZrO_2.[23] Although photoproduct **Int** (Figure 5) has not been identified, it is presumably a bpy-based intermediate with coordination of a single pyridyl arm and coordination of an anion from solution, ZrO_2-$[((OP(OH)O)_2bpy)Ru^{II}(bpy)(py\text{-}py)X^+$ (X = $^-OOCCH_3$, Cl^-, $SO_3CF_3^-$, etc.). On the basis of long-term spectral measurements, surface photochemical substitution is thermally reversible, Figure 4.

Oxygen-Independent Desorption from TiO_2. In addition to the processes mentioned above on ZrO_2 (1–3), the relatively low conduction band of TiO_2 (−0.5 vs NHE, pH 7)[19,29] allows for excited state electron injection from $Ru^{II}P$* (5) into the metal oxide, TiO_2-**RuP** + hν → TiO_2-$Ru^{II}P$* → $TiO_2(e^-)$-$Ru^{III}P$ (7). In the absence of oxygen, desorption rate for **RuP** on TiO_2 is more rapid than on ZrO_2 by a factor of 5, Table 1. Although desorption processes on the two surfaces may be similar, part of the enhanced rate of loss from TiO_2 may be attributable to a lower binding affinity of the phosphonate group for titanium versus zirconium. It has been shown that treatment of TiO_2 and other metal oxide surfaces with alkoxyzirconium compounds significantly increases the stability of surface bound alkanecarboxylates and phosphonates to both thermal and mechanical (washing, tape-based pealing) stress.[30] Alternatively, Uam et al. have suggested that $Ru^{III}P$ on $TiO_2(e^-)$ desorbs from the surface because of its lower formation constant than the $Ru^{II}P$ species on ZrO_2.[11] Also on TiO_2, excitation and injection are followed by highly favored back electron transfer, $TiO_2(e^-)$-$Ru^{III}P$ → TiO_2–$Ru^{II}P$ (8), with $\Delta G \approx -1.3$ eV. Local energy release into phonon modes with local heating may promote thermal desorption of **RuP**.

Oxygen-Dependent Desorption from TiO_2. In all solvents tested, a 4-fold or greater increase in k_{des} for TiO_2-**RuP** was observed in the presence of oxygen relative to an inert (argon or nitrogen) atmosphere. This result coincides with the observed decrease in device lifetime in the presence of oxygen.[13] Given the known ultrafast injection rates for adsorbed polypyridyl complexes,[31] desorption by sensitized formation of $^1O_2$ seems unlikely. Instead oxygen may intervene by electron transfer reduction of O_2 to give $O_2^{\bullet-}$ (6) in competition with back electron transfer to $Ru^{III}P$ (8). It has been demonstrated that after direct band gap excitation the electron in the conduction band of TiO_2 is sufficiently reducing to produce superoxide radicals and other reactive species.[32] Presumably a similar reductive pathway is available in these sensitized systems due to excited-state electron injection into the conduction band of TiO_2. Superoxide radicals ($O_2^{\bullet-}$) and other byproducts ($OH^{\bullet}$, H_2O_2, etc.) have been implicated in chemistry/catalysis at metal oxide surfaces.[32,33] The buildup of reactive radical or radical precursors and surface reactions may lead to desorption (7). Supporting this conclusion is the almost 10-fold increase in desorption rate of **RuP** from TiO_2 in both the dark ($k_{des} = 0.2 \times 10^{-5}$ s^{-1}) and under irradiation ($k_{des} = 46.9 \times 10^{-5}$ s^{-1}) in a 0.1 M $HClO_4$ aqueous solution with 5% H_2O_2 (see Figure S8 in the Supporting Information).

In the presence of oxygen, k_{des} is dependent on the solvent, increasing in the order MeOH ≈ MeCN < PC <pH 1 ≪ pH 7. The solvent dependence of k_{des} has previously been discussed as being dependent on solvent properties like solvent donor number, viscosity, and dielectric constant.[11,34] Observed trends in donor number and viscosity for the four solvents in Table S3

do not correlate with variations in k_{des}. However, decreased desorption rates are observed as the dielectric constant decreases in the order of: water (80) > PC (66) > MeCN (36) ≈ MeOH(33).[35] Given the mechanism discussion above, the dependence of k_{des} on solvent dielectric may reflect, in part, a change in the reactivity chemistry of $O_2^{\bullet-}$. A surface desorption mechanism based on local heating effects could also explain the solvent dependence as arising from different surface solvation energies as the complex is released.

The observed decrease in stability of TiO_2–**RuP** at higher pH values is in good agreement with previous reports.[6,9,21] Surface instability as the pH is increased is attributable to hydrolysis of the Ti–O–P/Ti–O–C surface bonds. The appearance of an implied base effect is consistent with a role for OH^- in the substitution process at individual surface sites.

Based on our results, desorption is negligible in the dark at pH 1 but is significantly enhanced by photolysis. The light and pH dependences of the desorption process suggest that either the excited state (TiO_2-$Ru^{II}P^*$) and/or $TiO_2(e^-)$-$Ru^{III}P$, reached by injection, promotes hydrolysis.

There may be an important contribution to the desorption process from pH-induced changes in the protonation state of the complex and/or surface. It has been shown that both TiO_2 nanoparticles and **RuP** behave as simple diprotic acids with $pK_{a1} = 5.0$, $pK_{a2} = 7.8$ and $pK_{a1} = 1$, $pK_{a2} = 6$ for TiO_2 and **RuP**, respectively.[36,37] Increasing the pH of the solution and deprotonation of the surface-bound complex/surface results in a negative charge buildup at the interface which may promote the desorption process(es). However, it is currently unclear how large of a role electrostatic charge has in the surface binding and stability.

The addition of salts to methanol has a significant but selective effect on the desorption rate. Addition of $LiOOCCH_3$ considerably increases the desorption rate of **RuP** from TiO_2. Alternatively, the addition of Cl^-, ClO_4^-, $SO_3CF_3^-$, or PF_6^- anions decrease the desorption rate. It is currently unclear as to the mechanism of stabilization in the presence of these ions. Electron donating anions like H_3CCOO^- are known to participate in ligand substitution reactions on TiO_2 replacing surface Ti–OH or Ti–OH_2 groups with H_3CCOO^-.[36] Surface substitution of **RuP** by H_3CCOO^- presumably plays a role here as well.

Photochemistry on TiO_2. Spectral changes with time, factoring out desorption to isolate the photochemical step, are suggestive of a one-step photochemical reaction, (3) in Figure 5. Although the identity of the surface photoproduct has not been definitively established, comparisons with the extensively investigated photochemistry of $[Ru^{II}(bpy)_3]^{2+}$ in solution provides useful insight.[38−40]

In solution, photoexcitation of $[Ru^{II}(bpy)_3]^{2+}$ results in rapid appearance of a lowest MLCT state, largely triplet in character (^{3}MLCT). Thermal activation and barrier crossing from ^{3}MLCT leads to population of a low lying d-d state or states. The change in electronic configuration between states is $(d\pi_{Ru})^5(\pi^*_{bpy})^1 \rightarrow (d\pi_{Ru})^5(d\sigma^*_{Ru})^1$. Given its antibonding character with regard to the metal–ligand bond, the d-d state can undergo thermally activated ligand loss and net substitution through a dissociative mechanism and a five coordinate intermediate with a singly bound bpy ligand, $[Ru^{II}(bpy)_2(py\text{-}py)]^{2+}$. Anion or solvent addition by substitution results in an intermediate species containing singly bound bpy, $[Ru^{II}(bpy)_2(py\text{-}py)(L)]^{2+}$, with L a solvent molecule or anion, X^{n-}. These monodentate bipyridine intermediates are usually unstable but long-lived intermediates (<10 min) of this type have been isolated and characterized.[40] The relatively short lifetime of these species is due to rechelation to regenerate $[Ru^{II}(bpy)_3]^{2+}$ or further substitution to give $Ru^{II}(bpy)_2X_2$.[39]

The reversibility and anion dependence of the appearance of the intermediate on the surface of TiO_2 are consistent with photosubstitution with **Int** in Figure 5, for example, as $[Ru^{II}(4,4'\text{-}(PO_3H_2)_2bpy)(bpy)(py\text{-}py)(OOCCH_3)]^+$ or perhaps a mixture of this intermediate and $Ru^{II}(4,4'\text{-}(PO_3H_2)_2bpy)(bpy)(OOCCH_3)_2$. This conclusion is consistent with the observed red-shift of the intense visible MLCT absorption band which is comparable to spectral shifts between $[Ru^{II}(bpy)_3]^{2+}$ and complexes of the type $[Ru^{II}(bpy)_2(pyridine)X]^+$.[28] The reversible nature of the spectral changes is consistent with the py-py complex as the intermediate, or at least as a coproduct. The spectral changes are insufficiently defining to make a distinction between the two possibilities.

The trend in k_{photo} with $H_3CCOO^- > Cl^- > ClO_4^- > SO_3CF_3^- > PF_6^-$, points to the importance of the coordinating ability of the anion with the traditionally noncoordinating anions, $SO_3CF_3^-$ and PF_6^-, providing a stabilization effect with regard to photosubstitution.[39] The lack of photoproduct(s) in aqueous solutions is consistent with the "self-annealing" behavior of $[Ru^{II}(bpy)_3]^{2+}$. In water, photosubstitution occurs but gives the aqua complex, $[Ru^{II}(bpy)_2(py\text{-}py)(OH_2)]^{2+}$ as intermediate. It undergoes chelate ring closure returning to $[Ru^{II}(bpy)_3]^{2+}$. In nonpolar, low dielectric solvents like CH_2Cl_2, initial ion-pairing induces substitution by capture of the intermediate through a proximity effect.[23]

There is a minimal cation dependence on k_{photo}. This is true even though electron injection yields are cation dependent with $\Phi_{inj} = 65–70\%$ for Mg^{2+} relative to $\Phi_{inj} = 35–40\%$ for Na^+ (1 mM).[41] Added O_2 has a negligible effect on k_{photo} as expected because of rapid injection once the excited state is formed.

Methodology. We have introduced a standardized measurement protocol for comparing the stability of $[Ru^{II}(bpy)_2(4,4'\text{-}(PO_3H_2)_2bpy)]^{2+}$ on metal oxides under a variety of conditions. There are limitations in the results. Rate constant measurements do not take into account minor spectral shifts associated with surface loading and intermolecular interactions that occur over the course of the experiment. The photolysis experiments were conducted with monochromatic radiation at 455 nm (30 nm fwhm) and there were no corrections for the fraction of light absorbed, limiting comparisons with systems having different absorption profiles. The photolysis conditions do not accurately reflect those found in most DSSC or DSPEC devices. The more than 135 times higher intensity of the 455 nm LED in these experiments (210 W $m^{-2}nm^{-1}$ at 455 nm), relative to the standard solar spectrum (1.53 W $m^{-2}nm^{-1}$ at 455 nm), increases the density of excited states and electron injection events. A comparison between the spectral irradiance of the AM 1.5G solar spectrum and the LED used in the stability measurements can be seen in Figure S9 in the Supporting Information. Moreover, these experiments were conducted under open circuit conditions without a reductant in solution. In an operating cell, electron collection and transfer to an external cathode would avoid desorption pathways induced by back electron transfer. The addition of a reductant (a catalyst in a DSPEC and redox mediator in DSSCs) would limit the lifetime of oxidized Ru^{III} species and thus inhibit any reaction pathway associated with this species.

CONCLUSIONS

In this manuscript, we have utilized, in a systematic way, a standard protocol to evaluate and compare the role of environmental effects on the photostability of surface bound $[Ru^{II}(bpy)_2(4,4'\text{-}(PO_3H_2)bpy)]^{2+}$. This includes conditions appropriate for water splitting, for example. Two surface loss processes were identified, desorption and photochemistry. The factors that influence these processes were investigated both on ZrO_2 and on TiO_2 with rapid electron injection from the excited state occurring on the latter.

Our results provide a benchmark for comparing surface binding, $-PO_3H_2$ versus $-COOH$, and the role of environmental variables (pH, solvent, electrolyte, etc.) in influencing the stability of surface binding over extended periods. Some overall conclusions regarding relative stability of surface bound chromophores emerge from our results:

- O_2 promotes desorption on both ZrO_2 and TiO_2 surfaces, seemingly by different mechanisms.
- On ZrO_2, decomposition may be induced by production of $^1O_2$ and on TiO_2 by production of $O_2^{\bullet-}$, both followed by chemical attack on the surface link or links.
- Photodecomposition by excitation and thermal population of low lying d−d states induces photochemical ligand loss in nonaqueous solvents.
- Photochemistry is favored in nonaqueous solvents with added coordinating anions and is minimized for the noncoordinating anions $O_3SCF_3^-$ and PF_6^-.
- Desorption may be induced by excited state decay or strongly exoergic back electron transfer which lead to local heating effects through activation of phonon modes.

ASSOCIATED CONTENT

Supporting Information

Selected time-dependent absorbance changes, tabulated rate constants, light intensity comparisons, and other supporting data. This material is available free of charge via the Internet at http://pubs.acs.org/.

AUTHOR INFORMATION

Corresponding Author

*E-mail: tjmeyer@unc.edu.

Notes

The authors declare no competing financial interest.

ACKNOWLEDGMENTS

This work was funded by the UNC Energy Frontier Research Center (EFRC) "Center for Solar Fuels", an EFRC funded by the U.S. Department of Energy, Office of Science, Office of Basic Energy Sciences, under Award DESC0001011, supporting M.K.B., J.J.C., and K.H. Funding for W.S. and C.G. was provided by the CCHF, an EFRC funded by the U.S. Department of Energy, Office of Science, Office of Basic Energy Sciences, under Award DE-SC0001298 at the University of Virginia. We acknowledge support for the purchase of instrumentation from UNC EFRC (Center for Solar Fuels, an Energy Frontier Research Center funded by the U.S. Department of Energy, Office of Science, Office of Basic Energy Sciences under award number DESC0001011) and UNC SERC ("Solar Energy Research Center Instrumentation Facility" funded by the U.S. Department of Energy Office of Energy Efficiency & Renewable Energy under award number DE-EE0003188).

REFERENCES

(1) Hagfeldt, A.; Boschloo, G.; Sun, L.; Kloo, L.; Pettersson, H. *Chem. Rev.* **2010**, *110*, 6595−6663. Peter, L. M. *J. Phys. Chem. Lett.* **2011**, *2*, 1861−1867. Grätzel, M. *J. Photochem. Photobiol., C* **2003**, *4*, 145−153.

(2) Wang, D.; Wang, G.; Zhao, J.; Chen, B. *Chin. Sci. Bull.* **2007**, *52*, 2012−2014.

(3) Hara, K.; Tachibana, Y.; Ohga, Y.; Shinpo, A.; Suga, S.; Sayama, K.; Sugihara, H.; Arakawa, H. *Sol. Energy Mater. Sol. Cells* **2003**, *77*, 89−103.

(4) Heimer, T. A.; D'Arcangelis, S. T.; Farzad, F.; Stipkala, J. M.; Meyer, G. J. *Inorg. Chem.* **1996**, *35*, 5319−5324.

(5) Gillaizeau-Gauthier, I.; Odobel, F.; Alebbi, M.; Argazzi, R.; Costa, E.; Bignozzi, C. A.; Qu, P.; Meyer, G. J. *Inorg. Chem.* **2001**, *40*, 6073−6079.

(6) McNamara, W. R.; R. C. S. III.; Li, G.; Richter, C.; Allen, L. J.; Milot, R. L.; Schmuttenmaer, C. A.; Crabtree, R. H.; Brudvig, G. W.; Batista, V. S. *Energy Environ. Sci.* **2009**, *2*, 1173−1175.

(7) Amirnasr, M.; Nazeeruddin, M. K.; Gratzel, M. *Thermochim. Acta* **2000**, *348*, 105−114. Ning, Z.; Zhang, Q.; Wu, W.; Pei, H.; Liu, B.; Tian, H. *J. Org. Chem.* **2008**, *73*, 3791−3797. Nguyen, H.; Ta, H. M.; Lund, T. *Sol. Energy Mater. Sol. Cells* **2007**, *91*, 1934−1942. Mee Jung, Y.; Park, Y.; Sarker, S.; Lee, J.-J.; Dembereldorj, U.; Joo, S.-W. *Sol. Energy Mater. Sol. Cells* **2011**, *95*, 326−331.

(8) Caramori, S.; Cristino, V.; Argazzi, R.; Meda, L.; Bignozzi, C. A. *Inorg. Chem.* **2010**, *49*, 3320−3328.

(9) Park, Y.; Lee, S.-H.; Kang, S. O.; Choi, W. *Chem. Commun.* **2010**, *46*, 2477−2479.

(10) Ogawa, M.; Sohmiya, M.; Watase, Y. *Chem. Commun.* **2011**, *47*, 8602−8604. Bae, E.; Choi, W.; Park, J.; Shin, H. S.; Kim, S. B.; Lee, J. S. *J. Phys. Chem. B* **2004**, *108*, 14093−14101.

(11) Uam, H.-S.; Jung, Y.-S.; Jun, Y.; Kim, K.-J. *J. Photochem. Photobiol., A* **2010**, *212*, 122−128.

(12) Tributsch, H. *Coord. Chem. Rev.* **2004**, *248*, 1511−1530.

(13) Tennakone, K.; Kumara, G. R. R. A.; Kottegoda, I. R. M.; Wijayantha, K. G. U. *Semicond. Sci. Technol.* **1997**, *12*, 128.

(14) Greijer, H.; Lindgren, J.; Hagfeldt, A. *J. Phys. Chem. B* **2001**, *105*, 6314−6320. Likodimos, V.; Stergiopoulos, T.; Falaras, P.; Harikisun, R.; Desilvestro, J.; Tulloch, G. *J. Phys. Chem. C* **2009**, *113*, 9412−9422. Grünwald, R.; Tributsch, H. *J. Phys. Chem. B* **1997**, *101*, 2564−2575.

(15) Lee, S.-H. A.; Abrams, N. M.; Hoertz, P. G.; Barber, G. D.; Halaoui, L. I.; Mallouk, T. E. *J. Phys. Chem. B* **2008**, *112*, 14415−14421.

(16) Song, W.; Glasson, C. R. K.; Luo, H.; Hanson, K.; Brennaman, M. K.; Concepcion, J. J.; Meyer, T. J. *J. Phys. Chem. Lett.* **2011**, *2*, 1808−1813.

(17) Brennaman, M. K.; Patrocinio, A. O. T.; Song, W.; Jurss, J. W.; Concepcion, J. J.; Hoertz, P. G.; Traub, M. C.; Murakami Iha, N. Y.; Meyer, T. J. *ChemSusChem* **2011**, *4*, 216−227.

(18) Durrant, J. R.; Haque, S. A.; Palomares, E. *Coord. Chem. Rev.* **2004**, *248*, 1247−1257.

(19) Katoh, R.; Furube, A.; Yoshihara, T.; Hara, K.; Fujihashi, G.; Takano, S.; Murata, S.; Arakawa, H.; Tachiya, M. *J. Phys. Chem. B* **2004**, *108*, 4818−4822.

(20) Wendt, S.; Matthiesen, J.; Schaub, R.; Vestergaard, E. K.; Lægsgaard, E.; Besenbacher, F.; Hammer, B. *Phys. Rev. Lett.* **2006**, *96*, 066107.

(21) Weisz, A. D.; Regazzoni, A. E.; Blesa, M. A. *Solid State Ionics* **2001**, *143*, 125−130. Péchy, P.; Rotzinger, F. P.; Nazeeruddin, M. K.; Kohle, O.; Zakeeruddin, S. M.; Humphry-Baker, R.; Grätzel, M. *J. Chem. Soc., Chem. Commun.* **1995**, 65−66.

(22) Trammell, S. A.; Wimbish, J. C.; Odobel, F.; Gallagher, L. A.; Narula, P. M.; Meyer, T. J. *J. Am. Chem. Soc.* **1998**, *120*, 13248−13249.

(23) Durham, B.; Caspar, J. V.; Nagle, J. K.; Meyer, T. J. *J. Am. Chem. Soc.* **1982**, *104*, 4803−4810.

(24) Li, W.; Gandra, N.; Courtney, S. N.; Gao, R. *Chem. Phys. Chem.* **2009**, *10*, 1789−1793.

(25) Fujishima, A.; Rao, T. N.; Tryk, D. A. *J. Photochem. Photobiol., C* **2000**, *1*, 1−21. Yates, J. T. Jr. *Surf. Sci.* **2009**, *603*, 1605−1612.

(26) Demas, J. N.; Harris, E. W.; McBride, R. P. *J. Am. Chem. Soc.* **1977**, *99*, 3547−3551.
(27) DeRosa, M. C.; Crutchley, R. J. *Coord. Chem. Rev.* **2002**, *233*−*234*, 351−371.
(28) Durham, B.; Walsh, J. L.; Carter, C. L.; Meyer, T. J. *Inorg. Chem.* **1980**, *19*, 860−865.
(29) Hagfeldt, A.; Graetzel, M. *Chem. Rev.* **1995**, *95*, 49−68.
(30) Gawalt, E. S.; Lu, G.; Bernasek, S. L.; Schwartz, J. *Langmuir* **1999**, *15*, 8929−8933. Purvis, K. L.; Lu, G.; Schwartz, J.; Bernasek, S. L. *Langmuir* **1999**, *15*, 7092−7096.
(31) Ardo, S.; Meyer, G. J. *Chem. Soc. Rev.* **2009**, *38*, 115−164.
(32) Hirakawa, T.; Nosaka, Y. *Langmuir* **2002**, *18*, 3247−3254. Cai, R.; Baba, R.; Hashimoto, K.; Kubota, Y.; Fujishim, A. *J. Electroanal. Chem.* **1993**, *360*, 237−245.
(33) Li, X.; Cubbage, J. W.; Jenks, W. S. *J. Org. Chem.* **1999**, *64*, 8525−8536. Cermenati, L.; Pichat, P.; Guillard, C.; Albini, A. *J. Phys. Chem. B* **1997**, *101*, 2650−2658.
(34) Fukui, A.; Komiya, R.; Yamanaka, R.; Islam, A.; Han, L. *Sol. Energy Mater. Sol. Cells* **2006**, *90*, 649−658.
(35) *CRC Handbook of Chemistry and Physics*, 92nd ed.; CRC Press: Boca Raton, FL, 2012.
(36) Hoffmann, M. R.; Martin, S. T.; Choi, W.; Bahnemann, D. W. *Chem. Rev.* **1995**, *95*, 69−96.
(37) Montalti, M.; Wadhwa, S.; Kim, W. Y.; Kipp, R. A.; Schmehl, R. H. *Inorg. Chem.* **2000**, *39*, 76−84. Zabri, H.; Gillaizeau, I.; Bignozzi, C. A.; Caramori, S.; Charlot, M.-F.; Cano-Boquera, J.; Odobel, F. *Inorg. Chem.* **2003**, *42*, 6655−6666. Watson, D. F.; Marton, A.; Stux, A. M.; Meyer, G. J. *J. Phys. Chem. B* **2004**, *108*, 11680−11688. Schindler, P. W.; Gamsjager, H. *Discuss. Faraday Soc.* **1971**, *52*, 286−288.
(38) Vaidyalingam, A.; Dutta, P. K. *Anal. Chem.* **2000**, *72*, 5219−5224. Gleria, M.; Minto, F.; Beggiato, G.; Bortolus, P. *J. Chem. Soc., Chem. Commun.* **1978**, 285a−285a.
(39) Campagna, S.; Puntoriero, F.; Nastasi, F.; Bergamini, G.; Balzani, V. *Top. Curr. Chem.* **2007**, *280*, 117−214.
(40) Tachiyashiki, S.; Nakamaru, K.; Mizumachi, K. *Chem. Lett.* **1992**, *7*, 1119−1122. Tachiyashiki, S.; Ikezawa, H.; Mizumachi, K. *Inorg. Chem.* **1994**, *33*, 623−625.
(41) Kelly, C. A.; Farzad, F.; Thompson, D. W.; Stipkala, J. M.; Meyer, G. J. *Langmuir* **1999**, *15*, 7047−7054.